LA-UR-16-27876
Approved for public release; distribution is unlimited.

Title: QED Based Calculation of the Fine Structure Constant

Author(s): Lestone, John Paul

Intended for: To be distributed to interested parties.
Web

Issued: 2016-10-13

LA-UR-16-xxxxx

QED Based Calculation of the Fine Structure Constant

J. P. Lestone
Computational Physics Division, Los Alamos National Laboratory
Los Alamos, NM 87545, USA
October 13th, 2016

Quantum electrodynamics is complex and its associated mathematics can appear overwhelming for those not trained in this field. Here, semi-classical approaches are used to obtain a more intuitive feel for what causes electrostatics, and the anomalous magnetic moment of the electron. These intuitive arguments lead to a possible answer to the question of the nature of charge. Virtual photons, with a reduced wavelength of ƛ, are assumed to interact with isolated electrons with a cross section of $\pi ƛ^2$. This interaction is assumed to generate time-reversed virtual photons that are capable of seeking out and interacting with other electrons. This exchange of virtual photons between particles is assumed to generate and define the strength of electromagnetism. With the inclusion of near-field effects the model presented here gives a fine structure constant of ~1/137 and an anomalous magnetic moment of the electron of ~0.00116. These calculations support the possibility that near-field corrections are the key to understanding the numerical value of the dimensionless fine structure constant.

DOI: PACS number(s) : 03.65.Sq.

I. Introduction

Quantum electrodynamics (QED) is one of the most successful and tested theories ever developed. It can be viewed as one of the pinnacles of human thought. Its development was not easy and it took several decades of concerted effort by many authors to obtain a working theory capable of giving precise predictions. The first steps to a usable theory of the interaction of matter and light, consistent with both special relativity and quantum mechanics, were taken by Dirac in the late 1920s [1,2]. Significant contributions by others followed, culminating in a series of papers by Tomonaga [3], Schwinger [4-6], Feynman [7-9], and Dyson [10,11]. Those trained in QED have since been able to calculate many experimental observables with extraordinary precision, given the fine structure constant obtained via experiment as an input. The fine structure constant, α, is defined relative to the elementary charge e via

$$e^2 = \alpha \hbar c\, 4\pi\varepsilon_o. \quad (1)$$

The electrostatic force between two electrons separated by a distance d can be expressed as

$$F = \frac{e^2}{4\pi\varepsilon_o d^2} = \frac{\alpha \hbar c}{d^2}. \quad (2)$$

Despite the central importance of the value of α to QED, and the many attempts to understand it from a theoretical perspective [12], there is still no accepted theory to explain its value [12] and the corresponding elementary charge e=1.602177×10^{-19} C.

Even though doable, precise QED calculations can still require monumental effort. For example, the anomalous magnetic moment of the electron, (g–2)/2, was first obtained by Schwinger to 2nd order, $\alpha/(2\pi)$, in 1947 [4]. Calculations to higher order required considerable effort. Exact 4th and 6th order corrections were not obtained until 1957 [13] and 1996 [14], respectively. Numerical estimates to 8th [15,16] and 10th [17] order have since been obtained. The theoretical relationship between (g–2)/2 and α, is now considered to be so strong, and the modern (g–2)/2 measurements so precise [18], that the modern estimate of α=1/137.0359991 [19] is inferred from (g–2)/2 measurements via QED theory.

In the present paper, we use semi-classical arguments without full quantum theory or detailed special relativity to enable those not trained in field theory to obtain a better intuitive feel for what causes electrostatics, and the anomalous magnetic moment of the electron. By their nature, semi-classical approximations of complex phenomena can be difficult to justify. Often, assumptions can only be justified by their ability to reproduce experimental observables, and to provide an intermediate picture on our journey to a more complete understanding of the phenomenon in question. One of the most famous examples of this is the Bohr Model of the hydrogen atom, which can accurately reproduce the corresponding atomic spectroscopy, and served as an intermediate step to the more complete picture obtainable via the Schrödinger Equation. However, the reader should be aware that the semi-classical calculations presented here are no substitute for full quantum field theory calculations, which form the cornerstone of our understanding of elementary particles and fields.

If the semi-classical recipes presented here only gave values consistent with results already obtainable via QED then they would only be of interest as potential teaching

tools to introduce some QED processes to an undergraduate audience. However, the concepts presented here lead to a possible answer to the question of the nature of charge. By invoking a far-field virtual-photon particle interaction cross section of $\pi\lambda\!\!\!^{-2}$, and the inclusion of near-field effects, a universal charge of 1.60×10^{-19} C emerges from the model.

II. Virtual Vacuum Photons

Assuming a large piece of vacuum of volume $V=L^3$ contained within a conducting cube, where L is the length of one of the cube's sides, many introductory QED text books derive the energy and/or number density of virtual photons in the infinite energy-density vacuum. This concept is central to the present work, and because one of our aims is to convey our semi-classical QED ideas to a wide audience, we re-derive the infinite energy-density virtual-photon vacuum here. Given the boundary condition of no electric field parallel to the surface of the conducting cube walls, the electric field in the x direction inside the cube is of the form

$$E_{n_x} = \sum_{n_x} E_{0nx} \sin(w_n t + \varphi_{n_x}) \times \sin(x / \lambda\!\!\!^{-}_{n_x}), \tag{3}$$

where the sum is over n_x=1 to ∞. The reduced wavelength in the x direction is given by

$$\lambda\!\!\!^{-}_{n_x} = \frac{\lambda_{n_x}}{2\pi} = \frac{L}{n_x \pi}. \tag{4}$$

The corresponding angular frequencies are given by $\omega_n=c/\lambda\!\!\!^{-}_n$, where c is the speed of light, and $\lambda\!\!\!^{-}_n$ is the reduced wavelength of the mode including any y and z components.

To determine the number of possible virtual modes with a fixed frequency (energy) we, for simplicity, first consider standing modes in the cube, moving along a vector in the xy plane at an angle α to the x direction and β to the y direction (see Fig. 1). In two dimensions it is easy to see that $\lambda_{nx}=\lambda_n/\cos(\alpha)$ and $\lambda_{ny}=\lambda_n/\cos(\beta)$. The addition of the third dimension introduces the third relationship $\lambda_{nz}=\lambda_n/\cos(\gamma)$ where γ is the angle of the mode direction to the z direction. The relationship between the three angles defining the direction of the mode is constrained by $\cos^2(\alpha) + \cos^2(\beta) + \cos^2(\gamma) = 1$. This relationship and the constraints defined by Eq. (4) lead to the result

$$\sqrt{n_x^2 + n_y^2 + n_z^2} = \frac{\omega_n L}{c\pi} = r_n. \tag{5}$$

In the limit of a very large cube where even the long wavelength modes are characterized by large n values, the number of modes from r_n to $r_n + dr_n$ is given by

$$N(r_n)dr_n = \frac{4\pi r_n^2 dr_n}{8} = \frac{\pi r_n^2 dr_n}{2}. \tag{6}$$

Using the relationship between r_n and ω_n gives

$$N(\omega_n)d\omega_n = \frac{\pi}{2}\left(\frac{L}{c\pi}\right)^3 \omega_n^2 d\omega_n. \tag{7}$$

Multiplying by two to include both planes of polarization, and dividing by the volume of the cube, gives the number density of the vacuum modes

$$\rho_N(\omega_n)d\omega_n = \frac{\omega_n^2 d\omega_n}{\pi^2 c^3}. \tag{8}$$

Setting the energy in each mode to the ground state (vacuum) value of $\hbar\omega/2$ gives the energy density

$$\rho_E(\omega_n)d\omega_n = \frac{\hbar\omega^3 d\omega}{2\pi^2 c^3}. \tag{9}$$

The infinite energy density is a consequence of the lack of an upper limit in the possible frequency of the modes.

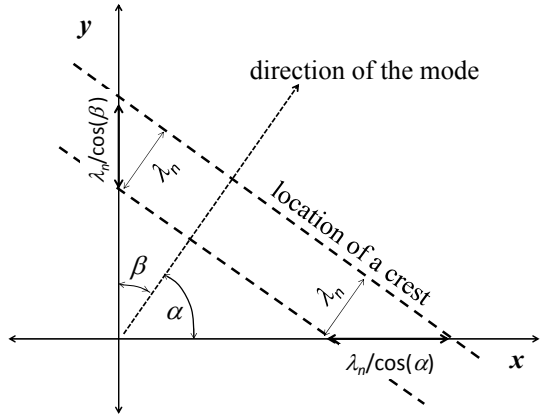

Fig. 1. Schematic diagram displaying the relationship between the wavelength of a mode in the xy plane to the corresponding values of λ_{nx} and λ_{ny}.

III. Stimulated Virtual Photons

For systems where the wavelength of the incident particle is very much larger than the geometric size of the target, and where the interaction potential varies slowly and smoothly and is always attractive, the interaction cross section is $\pi\lambda\!\!\!^{-2}$. We assume the same cross section for the production of stimulated virtual photons generated by the interaction of an isolated electron with the virtual-vacuum photons. The rate of stimulated virtual-photon production from an isolated electron can be determined by multiplying the number of vacuum photons in a shell of radius r and thickness dr surrounding an isolated electron by the probability that a photon originating from the shell will generate a stimulated emission. The corresponding number of generated (stimulated) virtual photons is given by

$$N_S(\omega) = \frac{\omega^2 d\omega}{\pi^2 c^3} 4\pi r^2 dr \frac{\pi\lambda\!\!\!^{-2}}{4\pi r^2} = \frac{d\omega\, dr}{\pi c}. \tag{10}$$

The time it takes the photons heading towards the electron, to clear the shell is $dt=dr/c$. Substituting this into Eq. (10) gives the rate of virtual photon generation

$$R_S(\omega) = \frac{N_S(\omega)}{dt} = \frac{d\omega}{\pi}. \tag{11}$$

This is a very simple and beautiful result that is central to the results that follow.

IV. Electrostatics

If a virtual-vacuum photon moving in the direction $-k$, with energy $\hbar\omega/2$, stimulates the production of a virtual photon in the opposite direction k, then the new photon must have an energy $\hbar\omega$. This is because the mode is already occupied with the ground-state energy of $\hbar\omega/2$. To accommodate the new photon, the energy in the mode will need to be increased by a full $\hbar\omega$ to obtain the next higher allowed energy of $3\hbar\omega/2$. The concept of time-reversed stimulated emission is borrowed from the properties of black holes [20]. Ignoring, for the present moment, conservation of energy and momentum, the power of the stimulated emission from an isolated electron is obtained by integrating over Eq. (11) multiplied by $\varepsilon = \hbar\omega$, and is given by

$$P_S = \int_0^\infty \frac{\hbar\omega d(\hbar\omega)}{\pi\hbar} = \int_0^\infty \frac{\varepsilon d\varepsilon}{\pi\hbar}. \tag{12}$$

Of course, this stimulated emission violates conservation of energy, and is not allowed from an isolated electron. However, a violation of conservation of energy by an amount ε can be allowed for a time scale given by the time-energy uncertainty principle, $\tau = \hbar/(2\varepsilon)$. If, in this time scale, the stimulated emission could find a partner electron, then conservation of energy can be re-established and the exchange of the stimulated emission between a pair allowed. We speculate that this exchange is the origin of the repulsive force between two electrons, and that the stimulated emission of virtual photons associated with an electron virtual-photon interaction cross section of $\pi\lambda\!\!\!^{-2}$ is the origin of the fundamental unit of electromagnetic charge, and thus the numerical value of the fine structure constant.

The time required for a virtual photon to be exchanged between a pair of electrons separated by a distance d is $t = d/c$. Assuming the probability per unit time that the virtual photon "disappears" is $2\varepsilon/\hbar = 1/\tau$, the probability that conservation of energy is allowed to be violated for the photon exchange time is $\exp(-t/\tau)$. Ignoring near-field effects, the power of the virtual exchange from electron A to electron B can be expressed as

$$P_{A\to B} = \frac{1}{\pi\hbar}\int_0^\infty \varepsilon \exp(-\frac{d}{c}\frac{2\varepsilon}{\hbar})\ \frac{\pi\lambda\!\!\!^{-2}}{4\pi d^2} d\varepsilon. \tag{13}$$

The $\pi\lambda\!\!\!^{-2}/(4\pi d^2)$ term is the assumed probability of finding the partner, assuming the jump across the distance d has been made. Given Eq. (13), the force generated by the two-way exchange of stimulated virtual photons is

$$\begin{aligned} F &= \frac{2}{\pi\hbar c}\int_0^\infty \varepsilon \exp(-\varepsilon/T_{\text{ex}})\ \frac{(\hbar c)^2}{4\varepsilon^2 d^2} d\varepsilon \\ &= \frac{\hbar c}{2\pi d^2}\int_0^\infty \frac{\exp(-\varepsilon/T_{\text{ex}})}{\varepsilon} d\varepsilon, \end{aligned} \tag{14}$$

where $T_{\text{ex}}=\hbar c/(2d)$ can be thought of as an effective exchange temperature. Instead of calculating the force directly, the energy stored in the exchanging stimulated virtual photons can be obtained as a function of the separation distance. The derivative of this potential energy can then be used to obtain the force. The corresponding results is the same as that given in Eq. (14). If this force is assumed to be the origin of electromagnetism, then the fine structure constant can be expressed as

$$\alpha = \frac{1}{2\pi}\int_0^\infty \frac{\exp(-\varepsilon/T_{\text{ex}})}{\varepsilon} d\varepsilon. \tag{15}$$

This integral diverges and gives an infinite strength for the repulsive force between two electrons. However, the origin of the divergence is the lowest-energy photons where $\lambda\!\!\!^{-} > d$, and where the interaction cross section needs to be modified to lower values to correct for near-field effects.

IV.A Near-field Effects

All classical antenna pairs emitting and absorbing radiation at a wavelength of λ experience strong near-field effects when separated by distances less than $\sim\lambda\!\!\!^{-}$ [21]. These effects are complex and manifest themselves as a reduced ability for the antenna pair to communicate with each other, and the potential for large amounts of near-field energy storage in the region within $\sim\lambda\!\!\!^{-}$ of the antenna pair. Even for simple classical systems, the near-field effects can be very difficult to predict. It is possible that the needed *e-e* (electron-electron) near-field effects can be calculated using classical electromagnetic theory. Here, we do not proceed down this path but instead start with the question of what is charge? In particular we need to determine why the properties of an isolated electron would be changed by the presence of a partner. In this paper, we have suggested that the fundamental unit of electromagnetic charge is associated with a far-field interaction cross section of $\pi\lambda\!\!\!^{-2}$ between particles and the virtual-vacuum photons. In the case of an isolated electron, the $\pi\lambda\!\!\!^{-2}$ cross section is assumed to be associated with the stimulated emission of virtual photons. These stimulated virtual photons must "disappear" or be absorbed within a time scale of $\hbar/(2\varepsilon)$. In this sense, electrons must be in a constant emission and disappearance and/or re-absorption dance with the stimulated virtual photons. An attempt to understand this process via semi-classical means is fraught with potential pit falls. However, an attempt is made here.

The stimulated virtual-photon electron dance mentioned above will produce a cloud of virtual photons surrounding electrons. For the stimulated virtual photons at a fixed frequency, it seems logical that their wave function should be of the form of the harmonic oscillator wave function $\psi(r) \propto \exp(-r^2/(2\sigma^2))$. But what value should be used for the relevant length scale? Given the assumed interaction cross section of $\pi\lambda\!\!\!^{-2}$ and the assumed presence of strong near-field corrections at a length scale less than $\sim\lambda\!\!\!^{-}$, the relevant simple

harmonic wave function length scale must be of the order of ƛ.

If the motion of the photon-electron dance was only in one dimension we could think of a classical harmonic cycle with the virtual photons going out a distance x_{max}, returning the same distance to the equilibrium position, overshooting a distance x_{max} on the opposite side and then completing the cycle by returning back to the equilibrium point. In this case, one cycle would be characterized by a total photon motion of $4x_{max}$. If this was the case then the correspondence between a classical 1D oscillator and the corresponding quantum oscillator would suggest $\sigma = x_{max}$. The value of x_{max} can be estimated by first noting that the emission of a photon of energy ε will lead to a maximum electron recoil kinetic energy of $K_{max}=\varepsilon^2/(2mc^2)$. If this is assumed to be associated with 1D harmonic motion of an electron with angular frequency ω, then the amplitude of the electron oscillation will be

$$x_{max}(e) = \frac{1}{\omega}\sqrt{\frac{2K_{max}}{m}} = \frac{\hbar}{mc} = r_C, \qquad (16)$$

where r_C, is the reduced Compton wavelength. If we assume a semi-classical effective photon mass of $p/c=\hbar\omega/c^2$, then by conservation of momentum the amplitude of the photon motion is given by

$$x_{max}(\gamma) = \frac{mc^2}{\hbar\omega}\frac{\hbar}{mc} = \frac{c}{\omega} = ƛ. \qquad (17)$$

However, instead of a semi-classical 1D photon oscillation with a constantly changing photon speed, it seems more intuitive to picture the virtual photon "orbiting" the electron at a constant speed and a radius such that the total distance travelled per orbit (cycle) is still $4x_{max}=4ƛ$. This sets a radius and wave function length scale of $\sigma = 2ƛ/\pi$. The reader should be aware that several seemingly logical choices exist to build a semi-classical picture of the virtual-photon electron dance. The presented choices are partially justified by the favorable outcomes generated later in this paper.

Given the above semi-classical suggestions, we assume that the fundamental unit of charge is associated with the cloud of virtual photons surrounding each charge unit with the wave function

$$\psi(r, ƛ)\,dv = \frac{\pi^{3/2}}{2^6 ƛ^3}\exp(\frac{-\pi^2 r^2}{8ƛ^2})\,dv. \qquad (18)$$

For a pair of electrons, we assume the combined interaction cross section of the pair scales with the square of the sum of the two wave functions, and is given by the volume integral

$$\sigma_{\gamma ee}(ƛ, d) = \pi ƛ^2 \int_v (\psi(\tilde{r}, ƛ) + \psi(\tilde{r} - \tilde{d}, ƛ))^2\,dv. \qquad (19)$$

This gives the known results for the two limits of large and small separation distances d, relative to ƛ. These results are: the two electrons act as two independent charges when $d \gg ƛ$; and act as a single charge of two units with four times the interaction cross section of a single electron when $d \ll ƛ$. To obtain an analytical expression for the near-field correction factor we first rewrite Eq. (19) as

$$\sigma_{\gamma ee}(ƛ, d) = 2\pi ƛ^2[1 + \int_v \psi(\tilde{r}, ƛ)\psi(\tilde{r} - \tilde{d}, ƛ)\,dv]. \qquad (20)$$

The integral

$$I(ƛ, d) = \int_v \psi(\tilde{r}, ƛ)\psi(\tilde{r} - \tilde{d}, ƛ)\,dv \qquad (21)$$

smoothly varies from zero to unity as the separation distance changes from ∞ to 0, and contains the influence of a partner that causes the interaction with the pair to be different from interactions that only sense the separate electrons. It is only the interactions that sense the separate electrons that have a possibility of generating a photon exchange. Virtual-vacuum photons that interact with the pair as a collective, generate stimulated virtual photons that are emitted from the pair and cause the pair to recoil as a collective, and cannot change the momentum of either electron relative to the other. The ability of a single electron in a pair to interact with a separate identity is thus given by the cross section

$$\sigma_S(ƛ, d) = \pi ƛ^2(1 - I(ƛ, d)). \qquad (22)$$

Given Eqs (18), (20), and (22) it is fairly straightforward to demonstrate that the near-field reduction factor that scales the isolated far-field interaction cross section is

$$f_{nf}(ƛ, d) = 1 - \exp(\frac{-\pi^2 d^2}{16 ƛ^2}). \qquad (23)$$

The relevant length scale for *e-e* near-field effects is $8^{1/2}ƛ/\pi \sim 9ƛ/10$. To modify the calculation of the fine structure constant given by Eq. (15) to include near-field effects, the cross section for the generation of stimulated virtual photons associated with the recoil of a single electron must be multiplied by f_{nf} to take into account the influence of the partner. Perhaps less obvious, is that the cross section used to calculate the probability of completing the exchange must also be multiplied by f_{nf}. This is due to time-symmetry arguments that apply equally to emission and absorption processes. Including the near-field effects at both the generation and completion end of the photon exchanges gives the result

$$\alpha = \frac{1}{2\pi}\int_0^\infty \frac{f_{nf}^2(ƛ, d)\exp(-\varepsilon/T_{ex})}{\varepsilon}\,d\varepsilon. \qquad (24)$$

However, this is not the final result because we assume that the absorption at the end of an exchange generates an additional time-reversed stimulated emission. Given the successful completion of the first exchange from electron *A* to electron *B*, the additional time-reversed photon is assumed to be heading in a direction to automatically re-find electron *A*. The probability of the exchange back is therefore only controlled by the need to continue to borrow the energy ε against the time-energy uncertainty principle. The continued following of this logic will cause the generation of yet additional exchanges between the electron pair with the probability of each additional exchange reduced by a factor of $\exp(-\varepsilon/T_{ex})$ (assuming a static system). This sequence of additional exchanges modifies Eq. (24). The

probability of the first exchange is proportional to $\exp(-\varepsilon/T_{ex})$, with the corresponding double exchange probability proportional to $\exp^2(-\varepsilon/T_{ex})$. If only single and double exchanges are considered then the probability of a single exchange not followed by an additional exchange will be proportional to $\exp(-\varepsilon/T_{ex})(1-\exp(-\varepsilon/T_{ex}))$. For this simplified case, the exponential factor in Eq. (24) needs to be replaced by

$$\begin{aligned} f_2 &= \exp(-\varepsilon/T_{ex})(1-\exp(-\varepsilon/T_{ex}))+2\exp^2(-\varepsilon/T_{ex}) \\ &= \exp(-\varepsilon/T_{ex})+\exp^2(-\varepsilon/T_{ex}). \end{aligned} \quad (25)$$

Following this logic, and including up to triple exchanges changes this factor to

$$f_3 = \exp(-\varepsilon/T_{ex})+\exp^2(-\varepsilon/T_{ex})+\exp^3(-\varepsilon/T_{ex}), \quad (26)$$

while allowing all possible additional exchanges leads to the factor

$$f_\infty = \frac{\exp(-\varepsilon/T_{ex})}{1-\exp(-\varepsilon/T_{ex})} = \frac{1}{\exp(\varepsilon/T_{ex})-1}. \quad (27)$$

The corresponding modification to Eq. (24) gives the result

$$\alpha_2 = \frac{1}{2\pi}\int_0^\infty \frac{(1-\exp(-\pi^2 d^2/(16\lambda\!\!\!^{-2})))^2}{\varepsilon(\exp(\varepsilon/T_{ex})-1)}\,d\varepsilon. \quad (28)$$

We have introduced a subscript 2 to signify this prediction is only to 2nd order, and does not include higher order terms (that must exist). At this point it is convenient to switch Eq. (28) into energy units of T_{ex}. This gives the more compact result

$$\alpha_2 = \frac{1}{2\pi}\int_0^\infty \frac{(1-\exp(-\pi^2\varepsilon^2/2^6))^2}{\varepsilon(\exp(\varepsilon)-1)}\,d\varepsilon. \quad (29)$$

This integral can be easily evaluated numerically (eg. by using Simpson's rule) giving the result α_2=1/142.078. The corresponding calculated charge is e_2= 1.57×10^{-19} C. The known value of α is close to $\alpha_2+5(\alpha_2)^2$. This is not inconsistent with the possibility that the difference between α and α_2 is associated with higher order corrections.

The force associated with the semi-classical exchange of virtual photons between two electrons represented by Eq. (29) can only generate repulsion. However, an attractive force between oppositely charged objects can be obtained by assuming the opposite charge is associated with a hole in a Fermi-sea of negative-energy particles [22]. Magnetism is not discussed here but falls out via Lorentz transformations between inertial frames.

V. Anomalous Magnetic Moment

The anomalous magnetic moment of the electron has been measured to extraordinary precision and is known to be $(g-2)/2$=0.001159652181 [23]. Precise measurements of both $(g-2)/2$ and the Lamb shift [24] have been used to test QED. For example, the electron-only QED calculation of $(g-2)/2$ can be written as [17]

$$\frac{g-2}{2} = \sum_{n=1}^{\infty} A_1^{(2n)}\left(\frac{\alpha}{\pi}\right)^n. \quad (30)$$

The first three $A_1^{(2n)}$ are known precisely and are $A_1^{(2)} = 0.5$, $A_1^{(4)} = -0.328478965579\ldots$, and $A_1^{(6)} = 1.1812456587\ldots$ Substituting α = 1/137.036 into Eq. (30) and using only terms with $n \le 3$ gives $(g-2)/2 = 0.00115965222$. The small difference from the measured value is due to a combination of even higher-order corrections, and non-electron and hadronic effects. Here, we are not looking for this level of accuracy but instead attempt to understand $(g-2)/2$ using semi-classical arguments.

To obtain a semi-classical recipe of $(g-2)/2$ we assume electrons are constantly stimulated to emit virtual photons whose energy is borrowed against the time-energy uncertainty principle. A consequence of this energy borrowing is that the stimulated virtual emission from an isolated electron must either disappear or be absorbed on a time scale of $\tau \sim \hbar/(2\varepsilon)$. After each emission, we assume the electron recoils with a velocity $v = \varepsilon/(mc)$ and curls in the external magnetic field with an orbital angular momentum of $\hbar$. The orientation of the orbital angular-momentum axis is assumed to be isotropic (like the incoming vacuum photons), but the handedness of the orbits are assumed to always be such that there is a positive component of the recoil-induced magnetic moment in the direction of the spin-induced magnetic moment of one Bohr-magneton. Given these assumptions, the average magnetic moment associated with the orbital motion of the recoiling electrons is one-half a Bohr magneton in the direction of the electron's spin. If this semi-classical picture is correct then the known 2nd order QED correction to the magnetic moment of electrons would imply electrons spend only α/π of their time in a state where recoils associated with the stimulated virtual-photon emission are generating the orbital magnetic moment discussed above.

In obtaining the estimate of the fine structure constant in the previous section, we assumed the stimulated virtual photons end their "lives" in one of two ways; they either "disappear", returning the borrowed energy, or re-establish conservation of energy and momentum by terminating in the partner electron. To obtain an estimate of $(g-2)/2$ we assume a third possibility: that the virtual photon can be self-absorbed. We further assume that the recoiling motion of the electron can only generate a magnetic moment if the recoiling electron self-absorbs the virtual photon. That is, the act of self-absorption is assumed to be the process by which the "virtual" recoil is transformed into a "real" recoil with measurable consequences to the magnetic moment. If the recoiling electron travels a distance δr around the circular orbit, then the corresponding elapsed time will be $\delta r \cdot mc/\varepsilon$. If all self-absorptions are assumed to occur after a travel distance of δr around the circular orbit then the fraction of time spent in a recoiling motion that ends with self-absorption can be obtained by multiplying the virtual-

photon emission rate by the elapsed time to self-absorption, and by the probability of a successful self-absorption. This probability can be obtained using the same logic used in the previous section but replacing the distance between the two electrons with the distance between the emission and self-absorption locations, Δr. This distance is different from the distance travelled around the assumed circular orbit δr. For typical self-absorptions, where the recoil only travels a small fraction of the possible circular path, the difference between δr and Δr is small. The above considerations lead to the fraction of time spent in a recoiling motion that ends with self-absorption

$$f_t = \int_0^\infty \frac{\partial r \cdot mc}{\varepsilon} \exp(\frac{-\varepsilon}{T_{sa}}) f_{nf}^2(\lambda\!\!\!^{-}, \Delta r) \frac{\pi \lambda\!\!\!^{-2}}{4\pi \Delta r^2} \frac{d\varepsilon}{\pi\hbar}. \qquad (31)$$

The effective self-absorption temperature is $T_{sa}=\hbar c/(2\Delta r)$. The exponential, in this case, is not replaced by Eq. (27), because only one electron is involved, and there is no pair for any additional stimulated emission to rattle between. Some simple algebraic manipulation and the switch to energy in units of T_{sa} gives

$$f_t = \frac{mc\partial r}{\pi\hbar} \int_0^\infty \frac{\exp(-\varepsilon)}{\varepsilon^3} \left(1 - \exp(\frac{-\pi^2\varepsilon^2}{2^6})\right)^2 d\varepsilon. \qquad (32)$$

Given the time-energy uncertainty constraints, the average distance travelled around the recoil orbit is $\delta r = \hbar/(2mc)$. Substituting this into Eq. (32) and multiplying by the one-half a Bohr-magneton generated by the randomly distributed orbits (as discussed above) gives an estimate of the anomalous magnetic moment of the electron

$$\frac{g_2 - 2}{2} = \frac{1}{4\pi} \int_0^\infty \frac{\exp(-\varepsilon)}{\varepsilon^3} \left(1 - \exp(\frac{-\pi^2\varepsilon^2}{2^6})\right)^2 d\varepsilon. \qquad (33)$$

We have introduced a subscript 2 to signify this prediction is only to 2nd order, and does not include higher order terms (that must exist). Eq. (33) can be easily evaluated numerically giving the result $(g_2-2)/2 = 0.0011423$. The known value of $(g-2)/2$ is close to $(g_2-2)/2 + 0.32\alpha^2$. This is not inconsistent with the possibility that the difference between $(g-2)/2$ and $(g_2-2)/2$ is associated with higher-order corrections. According to 2nd order QED, the ratio $(g-2)/(2\alpha) = 1/(2\pi)$. The corresponding value calculated via Eqs (29) and (33) is $(g_2-2)/(2\alpha_2) = 0.16234$. The corresponding value from 2nd order QED is close to $(g_2-2)/(2\alpha_2) - 0.44\alpha$. This is not inconsistent with the possibility of higher order corrections.

VI. Higher-order Corrections

The near-field correction term as expressed by Eq. (23) cannot be complete. There must be higher order correction terms associated with multiple reactions stemming from the passage of a single virtual-vacuum photon through the electron-pair system. Fig. 2 displays the functions inside the integrals in Eqs (29) and (33) along with the corresponding energy dependence of the near-field correction term $f_{nf}(\varepsilon)$ as given by Eq. (23). The function inside the $(g_2-2)/2$ integral expressed in Eq. (33) peaks at $\varepsilon \sim 0.8$ with an average of $\varepsilon \sim 1.3$. The function inside the α_2 integral given in Eq. (29) extends to larger values with a peak at $\varepsilon \sim 1.7$ with an average of $\varepsilon \sim 2.3$. To interpret these values, the reader is reminded that in Eqs (29) and (33) the units are such that $\varepsilon = 2$ corresponds to a separation distance between emission and absorption locations of $\lambda\!\!\!^{-}$. Notice that the near-field correction term starts to drop rapidly near $\varepsilon \sim 4$, where the separation distance is $\sim 2\lambda\!\!\!^{-}$. This is consistent with simple semi-classical overlap expectations, where each electron can be thought of as having an effective radius of $\lambda\!\!\!^{-}$ for its interaction with photons with a reduced wavelength of $\lambda\!\!\!^{-}$.

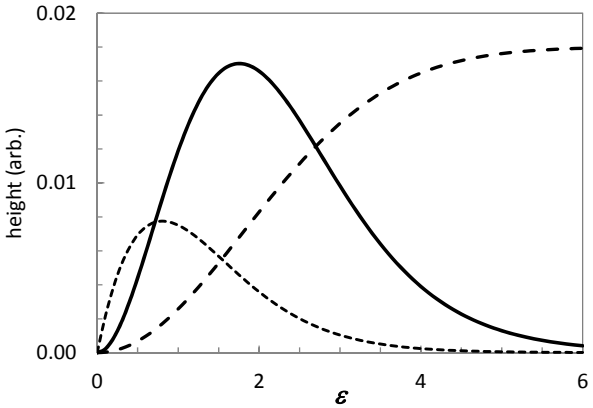

Fig. 2. The functions inside the integrals in Eqs (29) and (33) used to calculate α_2 (solid curve) and $(g_2-2)/2$ (short-dashed curve), along with the corresponding energy dependence of the near-field correction term $f_{nf}(\varepsilon)$ as given by Eq. (23) (long-dashed curve).

The calculations of α_2 and $(g_2-2)/2$ presented in sections IV and V are 3.5% and 1.5% lower, respectively, than the corresponding values inferred from experiment. If higher-order corrections to the near-field effects are to solve these discrepancies, then the near-field correction term $f_{nf}(\varepsilon)$ will need to be increased, and increased preferentially at $\varepsilon > 2$ in order to lift the α_2 calculation more than the $(g_2-2)/2$ calculation. This is exactly what is expected from higher-order corrections to the near-field effects. To see this, first consider two electrons separated by $\sim 2\lambda\!\!\!^{-}$ ($\varepsilon \sim 4$). In this case, the interaction of the vacuum photons will be predominately with either electron *A* or electron *B*. However, in the region between the two electrons, where the two wave functions overlap a little, the vacuum photons can generate stimulated-virtual emissions that cause the electron pair to recoil collectively. The strength of this collective interaction is governed by the $\exp(-\pi^2\varepsilon^2/2^6)$ term in Eq. (23). However, on their exit from the system, some fraction of the stimulated photons associated with collective recoils pass through regions where there is very little wave function overlap. This can lead to additional stimulated emission from either electron *A* or *B*. This higher order effect will

reduce the size of near-field corrections where the corrections are already small. We here denote the fraction of initially collective recoils that are followed by additional stimulated emissions associated with the recoil of an individual electron, as a. This would cause the near-field correction to be

$$f_{\rm nf}(\varepsilon) \sim 1 - \exp(\frac{-\pi^2\varepsilon^2}{2^6}) + a\exp(\frac{-\pi^2\varepsilon^2}{2^6}) , \qquad (34)$$

when $\varepsilon \sim 4$.

In the case of an electron pair with a separation distance $\ll$ ƛ, the near-field corrections are large because the wave function overlap is almost complete. This almost complete overlap means that the exiting stimulated photons associated with collective recoils will have a low probability of inducing any additional interactions associated with individual recoils. This means that if the near-field corrections are strong, they will be little modified by higher-order effects. To connect smoothly between Eq. (34) at $\varepsilon \sim 4$ and the low energy limit as given by Eq. (23), while maintaining the limit of $f_{\rm nf} \to 1$ as $\varepsilon \to \infty$, we suggest, in the absence of detailed higher-order calculations, the functional form

$$f_{\rm nf}(\varepsilon) = 1 - \exp(\frac{-\pi^2\varepsilon^2}{2^6}) + a\left(1 - \exp(\frac{-\pi^2\varepsilon^2}{2^6})\right)^b \exp(\frac{-\pi^2\varepsilon^2}{2^6}) . \qquad (35)$$

The two parameters can be tuned to a = 0.493788 and b = 4.709541 = 1.49909π to reproduce the known values of α and (g–2)/2. We do not know if any significance should be placed on the closeness of these values to ½ and 3π/2. The corresponding tuned $f_{\rm nf}$ is compared to the first-order calculation in Fig. 3 along with the difference (the higher-order correction). The highest corrections are near $\varepsilon \sim 3.4$ and thus corresponds to a separation distance of ~1.7ƛ.

Estimates of a and b can be made without any input from experiment by using the QED predicted relationship between (g–2)/2 and α given by Eq. (30). We here solve for allowable combinations of a and b using

$$\frac{g_4 - 2}{2} = \frac{\alpha_4}{2\pi} - 0.328478965579\ldots\left(\frac{\alpha_4}{\pi}\right)^2 + 1.1812456587\ldots\left(\frac{\alpha_4}{\pi}\right)^3 , \qquad (36)$$

where α_4 and (g_4–2)/2 are as defined by Eqs (29) and (33), but with the near-field correction term as given by Eq. (35). The allowed combinations of a and b are displayed in Fig. 4. On the right-hand-side of the minimum where a increases with increasing b, the higher-order corrections are largest in the region around $\varepsilon \sim 3$ to 4 (as expected), and leave the behavior at low ε alone. However, on the left-hand-side of the minimum, the apparent solutions cause the higher-order corrections to propagate down to low ε, and modify the low energy behavior away from the expectation discussed above. For this reason, the apparent solutions to the left of the minimum in Fig. 2 are rejected. In this rejected region, even though the apparent solutions are consisted with the QED relationship between (g–2)/(2) and α, as given by Eq. (30), the corresponding individual values are far from the known ones.

Without detailed calculations some limits can be placed on the size of the higher-order corrections and thus place limits on the allowable values of the parameters a and b. Based on the assumed far-field interaction cross section of πƛ^2, an isolated electron can, in a semi-classical sense, be viewed as a simple sphere of radius ƛ when interacting with photons with a reduced wavelength of ƛ. Therefore, from simple semi-classical overlap arguments (as discussed earlier) we expect the near-field correction to grow rapidly as the separation distance decreases through 2ƛ ($\varepsilon = 4$). This location is important for setting the size of the higher-order corrections because, as discussed earlier, the corrections will get smaller as the overlap grows with decreasing separation, and at larger separation the higher-order corrections will make little difference as $f_{\rm nf} \to 1$. But how big are they at the critical location?

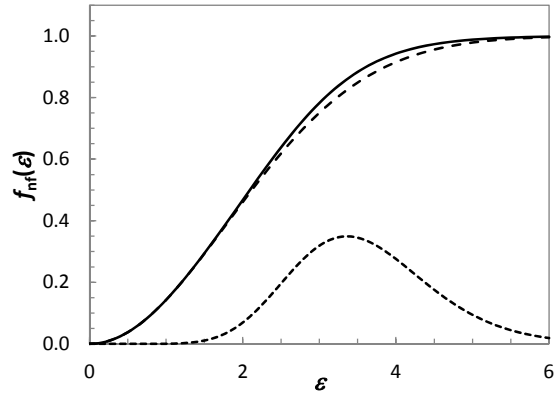

Fig. 3. The near-field correction term $f_{\rm nf}(\varepsilon)$ as given by Eq. (23) (long-dashed curve), and as given by Eq. (35) with a = 0.493788 and b = 4.709541 (solid curve). The short-dashed curve displays the difference multiplied by 10.

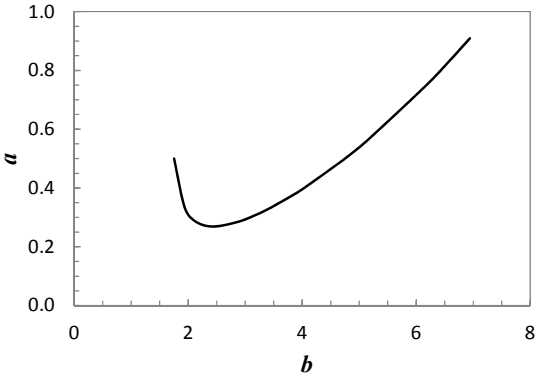

Fig. 4. The locus of the parameters a and b that reproduce the QED predicted relationship between (g_4–2)/2 and α_4.

An upper limit to the fraction a of stimulated virtual-photon emissions involved in collective recoils that subsequently generate stimulated virtual-photon emission

involving the recoil of one of the electrons, can be estimated by considering two touching (or barely overlapping) spheres both of radius ƛ. This is a crude surrogate for an electron pair separated by a distance 2ƛ. The far-field cross section is associated with the standard distribution of impact parameters corresponding to an average path length through the spheres of 4ƛ/3. In the simplified case considered here, only the overlap region between the spheres can generate collective interactions. The corresponding stimulated emission will diverge from this point, travelling through the spheres on either side. The average path length through the spheres of these diverging rays is ƛ. If the probability of an interaction were proportional to the average path length then the value of a would be ¾. Of course, the real situation is more complex, and will involve multiple dimensional integrals, and not a simple ratio of averages. The simple-sphere based estimate assumes the interaction is uniform and strong out to a radius ƛ, and then abruptly transitions to no interaction at larger radii. This causes an overestimate of the interaction strength of rays nearly parallel to the spheres. The factor of ¾ is thus likely an overestimate of the parameter a. However, it is difficult to understand how this estimate could be out by more than a factor of two. This sets an approximate lower bound of $a > 3/8$. Obviously limits and uncertainties are easier to set, and with great confidence, when the desired results are known. Given this, the quoted limits on a should be heavily scrutinized when more detailed work on *e-e* near-field effects becomes available. Figures 5 and 6 show the calculated $1/\alpha_4$ and $(g_4-2)/2$ as a function of the parameter a. Applying the limits $3/8 < a < 3/4$ leads to the estimates: the fine structure constant $\alpha_4 = 1/(137.0\pm0.6)$; and the anomalous magnetic moment of the electron $(g_4-2)/2 = 0.001160 \pm 0.000005$. The corresponding calculated fundamental unit of charge is $(1.6025 \pm 0.0033) \times 10^{-19}$ C.

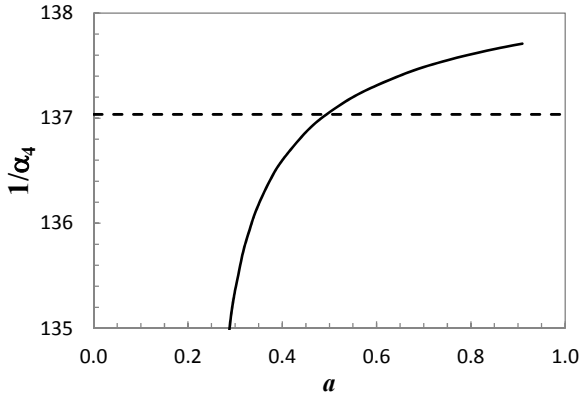

Fig. 5. The calculated $1/\alpha_4$ as a function of the parameter a (solid curve). The horizontal-dashed line displays the value of $1/\alpha$.

If we further speculate that both Eqs (29) and (33) should be modified by the same scaling factor, then this factor can be inferred from the ratio of the known $(g-2)/2$ to the calculated $(g_4-2)/2$. We can then write the corresponding estimate for the fine structure constant as

$$\alpha_6 = \frac{g-2}{g_4-2}\alpha_4 . \tag{37}$$

Fig. 7 shows the calculated $1/\alpha_6$ as a function of the parameter a. Applying the same limits as used before gives $\alpha_6 = 1/(137.0359\pm0.0009)$ and an inferred fundamental unit of charge of $(1.602177 \pm 0.000005) \times 10^{-19}$ C. This last result uses the known experimental value of $(g-2)/2$, and may be fortuitous. This result should not be used as strong evidence that Eqs (29) and (33) should be modified by the same scaling factor, but documented here because this suggestion should not be ruled out at the present time.

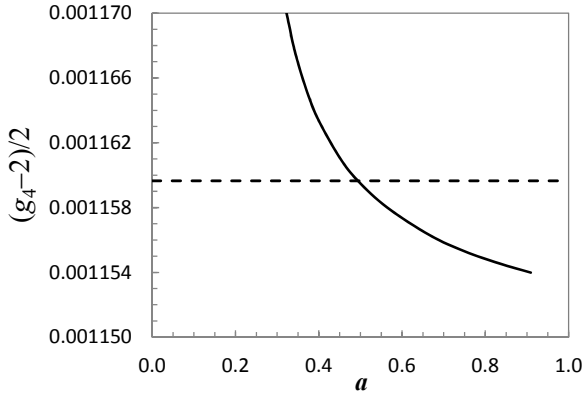

Fig. 6. The calculated $(g_4-2)/2$ as a function of the parameter a. The horizontal-dashed line displays the corresponding known value from experiment.

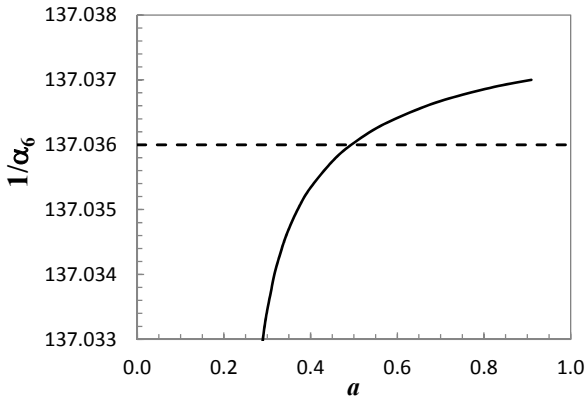

Fig. 7. $1/\alpha_6$ as a function of the parameter a (solid curve). The horizontal-dashed line displays the value of $1/\alpha$.

VII. Summary

Using semi-classical approaches, estimates for the fine structure constant and the anomalous magnetic moment of the electron can be made using intuitive steps that could be easily explained to an undergraduate physics audience. These steps involve a combination of stimulated virtual-photon emission, associated recoil effects, and absorption to re-establish conservation of energy and momentum on a

time scale consistent with the time-energy uncertainty principle.

Our first semi-classical estimate of the repulsive force generated by the exchange of virtual photons between a pair of electrons, obtained using only the far-field estimate of the virtual-photon electron interaction cross section of $\pi\lambda\!\!\!^{-2}$, is infinite. Including an estimate of near-field effects (to low order) obtained by wave function overlap arguments, partially justified by the $(g–2)/2$ calculation presented in section V, removes the divergence, leads to a force that is inversely proportional to the square of the separation distance, and gives an estimate of α_2 = 1/142.078. An estimate of $(g–2)/2$ obtained using the same near-field correction term is $(g_2–2)/2$ = 0.0011423. An estimate of higher-order corrections to near-field effects leads to the predictions $1/\alpha_4$=137.0±0.6 and $(g_4–2)/2$ = 0.001160 ± 0.000005. These values are in agreement with the known values obtained via experiment. Given these results, it is difficult to dismiss the idea that *e-e* near-field corrections are the key to understanding the numerical value of the dimensionless fine structure constant.

The nature of the photon exchange suggested here is QED based, with the photons involved being virtual, and with the dominant exchange photons having $\lambda\!\!\!^{-} \sim d$. In a semi-classical sense, this means the energy, path, and direction of an individual exchange are not definable. It would thus not be surprising in a more detailed quantum mechanical calculation that the details of the semi-classical exchange suggested here are lost, and the only surviving property is a single coupling constant. Only a static configuration of a pair of electrons is considered here. It would be interesting to consider the possibility of the generation of "real" photons in an extension of the presented scenario to a dynamical particle pair and/or triplet.

The predicted value of $1/\alpha_4$=137.0±0.6 corresponds to a predicted fundamental unit of charge of $(1.6025 \pm 0.0033) \times 10^{-19}$ C. These are accurate to 3 significant digits. However, the list of assumptions needed to obtain this result is long. These include: a far-field cross section of $\pi\lambda\!\!\!^{-2}$ for the generation of time-reversed stimulated virtual-photon emission; a harmonic oscillator wave function with a length scale set assuming circular "virtual" photon orbits; a probability per unit time that stimulated virtual photons "disappear", set by the time-energy uncertainty principle; a handedness of the circular orbits of the recoiling electrons such that there is always a positive component of the induced magnetic moment in the direction of the electron's spin; and a near-field correction term with higher-order corrections as given by Eq. (35) with only crude limits set for the parameter *a*. Obviously, more work on *e-e* near-field corrections is needed.

If the presented speculations are confirmed, the implications are too numerous to be discussed here. However, an important one is that the strength of electromagnetism would be controlled by simple geometrical factors and QED corrections, and α would be a mathematical constant like π and *e*, and not a physical one, at least in flat space-time and in the non-relativistic limit.

This work was supported in part by the U.S. Department of Energy.

[1] P.A.M Dirac, Proc. Roy. Soc. (London) **A114**, 243 (1927).
[2] P.A.M Dirac, Proc. Roy. Soc. (London) **A117**, 610 (1928).
[3] S. Tomonaga, Prog. Theor. Phys. **1**, 27 (1946).
[4] J. Schwinger, Phys. Rev. **73**, 416 (1948).
[5] J. Schwinger, Phys. Rev. **74**, 1439 (1949).
[6] J. Schwinger, Phys. Rev. **76**, 790 (1949).
[7] R. P. Feynman, Phys. Rev. **76**, 769 (1949).
[8] R. P. Feynman, Phys. Rev. **76**, 749 (1949).
[9] R. P. Feynman, Phys. Rev. **80**, 440 (1950).
[10] F. Dyson, Phys. Rev. **75**, 486 (1949).
[11] F. Dyson, Phys. Rev. **75**, 1736 (1949).
[12] U. D. Jentschura and I. Nandori, Eur. Phys. J. H, **39**, 591 (2014).
[13] A. Petermann, Helv. Phys. Acta, **30**, 407 (1957).
[14] S. Laporta and E. Remiddi, Phys. Lett. B, **379**, 283 (1996).
[15] T. Kinoshita and M. Nio, Phys. Rev. D **73**, 013003 (2006).
[16] T. Aoyama, M. Hayakawa, T. Kinoshita, and M. Nio, Phys. Rev. Lett. **99**, 110406 (2007).
[17] T. Aoyama, M. Hayakawa, T. Kinoshita, and M. Nio, Phys. Rev. D **85**, 033007 (2012).
[18] G. Gabrielse, D. Hanneke, T. Kinoshita, M. Nio, and B. Odom, Phys. Rev. Lett. **97**, 030802 (2006) and **99**, 039902 (2007).
[19] P. J. Mohr et al., http://physics.nist.gov/constants (2015), National Institute of Standards and Technology, Gaithersburg, MD 20899, USA.
[20] J. D. Bekenstein and A. Meisels, Phys. Rev. D, **15**, 2775 (1977).
[21] Z. Irahharten et al., IEEE International Conference on Communication, 2008, pg. 4872.
[22] J. D. Bjorken and S. D. Drell, Relativistic Quantum Mechanics, McGraw-Hill ISBN 07-005493-2 (1964).
[23] D. Hanneke, S. Fogwell Hoogerheide, and G. Gabrielse, Phys. Rev. A **83**, 052122 (2011).
[24] W. E. Lamb and R. C. Retherford, Phys. Rev. **72**, 241 (1947).